

## Laser ablation of bicomponent systems: A probe of molecular ejection mechanisms

Yaroslava G. Yingling,<sup>a)</sup> Leonid V. Zhigilei,<sup>b)</sup> and Barbara J. Garrison<sup>c)</sup>

152 Davey Laboratory, Department of Chemistry, The Pennsylvania State University, University Park, Pennsylvania 16802

Antonis Koubenakis,<sup>d)</sup> John Labrakis,<sup>e)</sup> and Savas Georgiou<sup>f)</sup>

Institute of Electronic Structure and Laser, Foundation for Research and Technology-Hellas, 71110 Heraklion, Crete, Greece

(Received 5 September 2000; accepted for publication 8 January 2001)

A combined experimental and molecular dynamics simulation study of laser ablation of a model bicomponent system with solutes of different volatility provides a consistent picture of the mechanisms of material ejection. The comparison of the ejection yields shows that there are two distinct regimes of molecular ejection, desorption at low laser fluences, and a collective ejection of a volume of material or ablation at higher fluences. Ejection of volatile solutes dominates in the desorption regime, whereas nonvolatile solutes are ejected only in the ablation regime. © 2001 American Institute of Physics. [DOI: 10.1063/1.1353816]

Material ejection from organic solids due to laser irradiation has important applications including those in mass spectrometry [matrix assisted laser desorption ionization (MALDI)],<sup>1</sup> thin polymer film deposition (matrix assisted pulsed laser evaporation),<sup>2</sup> and dry image production (laser ablation transfer).<sup>3</sup> Although the fundamental events involved are complex, there is a consensus developing among experimental and theoretical efforts as to the nature of the material removal processes. In particular, the results of our molecular dynamics (MD) simulation studies<sup>4–6</sup> predict the existence of two distinct regimes of molecular ejection, namely desorption at low laser fluences and ablation at higher fluences. This prediction is supported by MALDI experiments<sup>7</sup> of yields of ionic analyte molecules and neutral matrix molecules vs fluence that indicate entrainment of large molecules only above the ablation threshold;<sup>8,9</sup> calculations<sup>4–6,10</sup> and experimental data on cluster distributions vs fluence;<sup>11,12</sup> photoacoustic measurements;<sup>13</sup> and ablation studies of photoproducts.<sup>14,15</sup>

Further progress in the mechanistic understanding of laser ablation/desorption can be obtained from a direct comparison of experimental and simulation results for carefully designed systems. In this communication, we present the results of a combined experimental and simulation study of laser interaction with bicomponent molecular solids designed specifically to probe the mechanisms of material removal. Experiments are performed on several systems consisting of toluene, C<sub>6</sub>H<sub>5</sub>CH<sub>3</sub>, an UV-absorbing compound, as the dominant component (the matrix) and of a nonabsorbing compound as the second component (solute). We have cho-

sen to discuss in this letter two solutes, dimethyl ether, (CH<sub>3</sub>)<sub>2</sub>O, and decane, C<sub>10</sub>H<sub>22</sub>, that are more and less volatile than toluene, respectively, thus ensuring that relative desorption yields give a clear indication of the mechanisms of material ejection. For convenience, we refer to the two solutes as volatile and nonvolatile although only their volatility relative to toluene is important. Using electron impact ionization, the amount of each neutral component in the ejected plume from the corresponding mixtures is quantitatively measured.

The experimental setup is described in detail elsewhere.<sup>14,16</sup> Briefly, solids (~50 μm thick) are grown by condensation of introduced gases on a suprasil substrate at  $T \approx 100$  K. The solids were irradiated by the weakly focused (2 × 10 mm<sup>2</sup>) output of a KrF excimer laser (Lambda-Physik EMG150, λ = 248 nm, τ<sub>pulse</sub> ≈ 30 ns). For the dimethylether system, the signals are generally probed on a pulse-to-pulse basis, but at low fluences (<70 mJ/cm<sup>2</sup>), averaging over 10 pulses is necessary for good quality spectra. For the decane system, each point in the spectrum for fluences below 250 mJ/cm<sup>2</sup> is an average over 5–10 pulses. For the intensity determinations, corrections for the transit time of the ions through the mass spectrometer and for ionization efficiency of the neutral molecules have been discussed previously in Ref. 14.

All substances (Aldrich) are of high purity (99.5% or better) and are further distilled. Samples are prepared by pre-mixing of the vapors in a tank. To ensure a good signal-to-noise ratio in the detection, a molar concentration of solute of 17% (1:5 ratio) was employed.

The MD simulations of laser ablation of organic solids are performed using the breathing sphere model that is described elsewhere.<sup>8</sup> The essential feature of the model is an internal breathing mode for maintaining reasonable rates of energy transfer from the absorbing molecule to its neighbors. The solute molecules are introduced and homogeneously mixed with matrix molecules at a 10% concentration. The mass of all the molecules is 100 Daltons.

<sup>a)</sup>Electronic mail: yara@chem.psu.edu

<sup>b)</sup>Present address: Department of Materials Science and Engineering, Thornton Hall, University of Virginia, Charlottesville, VA 22903.

<sup>c)</sup>Electronic mail: bjg@psu.edu

<sup>d)</sup>Also at: Department of Physics, University of Crete, Greece.

<sup>e)</sup>Also at: Department of Chemistry, University of Crete, Greece.

<sup>f)</sup>Also at: Department of Physics, University of Ioannina, 45110 Ioannina, Greece; electronic mail: sgeorgiou@iesl.forth.gr

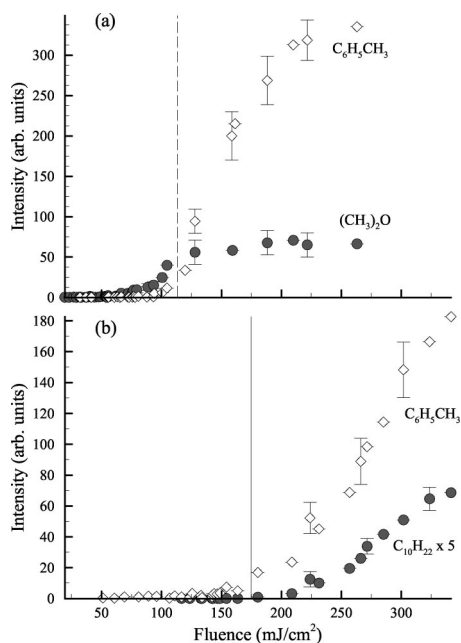


FIG. 1. Experimental desorption intensities for the (a)  $(\text{CH}_3)_2\text{O}/\text{C}_6\text{H}_5\text{CH}_3$  systems and (b)  $\text{C}_{10}\text{H}_{22}/\text{C}_6\text{H}_5\text{CH}_3$  as a function of laser fluence. The error bars represent  $2\sigma$ , as determined from five different measurements. The vertical lines indicate the approximate position of the ablation threshold.

Adjusting the well depth of the intermolecular pair potential controls the volatility of the solute molecules.<sup>8</sup> For the volatile and nonvolatile solutes, the binding energy of the solute molecule in the matrix is 0.45 and 0.92 eV, corresponding to an average cohesive energy of the systems of 0.57 and 0.66 eV/particle, respectively. The laser irradiation of 248 nm is deposited into the kinetic energy of the internal vibration of molecules chosen randomly following a Beer's law absorption probability. The size of the system ( $10 \times 10 \times 180$  nm), the laser pulse width (150 ps) and penetration depth (55 nm) are chosen to be the same as used in a study in which extensive comparisons were made to UV MALDI experimental results.<sup>5,6,17</sup>

The yields of molecules ejected from the  $(\text{CH}_3)_2\text{O}/\text{C}_6\text{H}_5\text{CH}_3$  and  $\text{C}_{10}\text{H}_{22}/\text{C}_6\text{H}_5\text{CH}_3$  mixtures upon laser irradiation at 248 nm are shown in Fig. 1. These two sets of data represent the range of results obtained for a number of different solutes.<sup>18</sup> Qualitatively, at low fluence the yield of molecules in the plume is low. As the fluence increases, there is threshold for ablation denoted by a steep increase in yield.

In order to highlight the effect of volatility on the efficiency of molecular ejection, the data of Fig. 1 are replotted in Fig. 2(a). Given are the percent concentrations of the solutes in the plume versus fluence. Clearly, in the low fluence regime, the plume from the  $(\text{CH}_3)_2\text{O}/\text{C}_6\text{H}_5\text{CH}_3$  system has an abundance of the volatile  $(\text{CH}_3)_2\text{O}$  molecules. A similar observation was made previously in the study of the  $c\text{-C}_3\text{H}_6/\text{C}_6\text{H}_5\text{CH}_3$  system.<sup>14</sup> In contrast, there is hardly any solute desorption at these fluences in the case of the  $\text{C}_{10}\text{H}_{22}/\text{C}_6\text{H}_5\text{CH}_3$  mixture. Above the corresponding ablation thresholds, both volatile and nonvolatile species are ejected efficiently.

The results of the simulations are presented in a similar form in Fig. 2(b). The computational results qualitatively

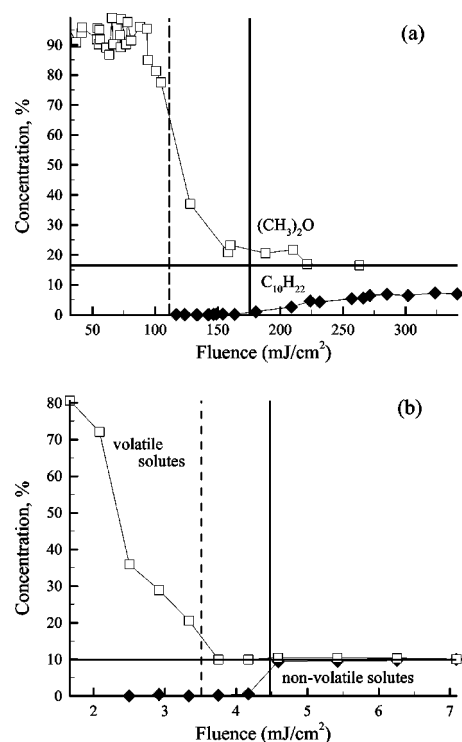


FIG. 2. Concentration of volatile and nonvolatile solutes in the plume vs laser fluence from (a) mass-spectrometric measurements and (b) molecular dynamics simulations. The horizontal lines indicate the initial concentration of solutes in the sample.

agree with the experimental observations and show the difference in desorption intensities and ablation thresholds for the systems with volatile and nonvolatile solutes. Although a full discussion of the relative values<sup>5,6</sup> of the fluence threshold for each curve is beyond the scope of this letter, both the experimental and calculated values show that the ablation thresholds vary with cohesive energy in the system. Quantitatively, the fluence values in the simulation differ by an order of magnitude from the experimental ones due to differences in the optical penetration depth, specific heat capacity,<sup>5</sup> no reflection losses in the simulations, etc.<sup>19</sup>

The presence of two mechanisms of material ejection is evident in the data given in Fig. 2. For the  $(\text{CH}_3)_2\text{O}/\text{C}_6\text{H}_5\text{CH}_3$  system, the solute dominates the plume at low fluences, even though its concentration in the original film is only 17%. As shown in earlier experiments<sup>20</sup> and simulations,<sup>21</sup> the molecules are ejecting from a liquid state. The high concentration in the plume can be explained by the volatile solutes diffusing toward the surface and desorbing more easily than the matrix molecules. The higher solute desorption concentration in the experiment [Fig. 2(a)] than in the simulation [Fig. 2(b)] may be attributed to the difference in the irradiation conditions. Longer pulses and multipulse irradiation protocols used in the experiments are expected to promote the diffusion and desorption of the volatile molecules. The high cohesive energies of nonvolatile solutes result in their negligible desorption at low laser fluences in both experiment and simulation [Fig. 2]. In contrast to the desorption regime, efficient ejection of the solutes in the ablation regime is observed reflecting the volume ejection nature of ablation.<sup>5,6</sup>

The experimental yield of decane in the ablation regime

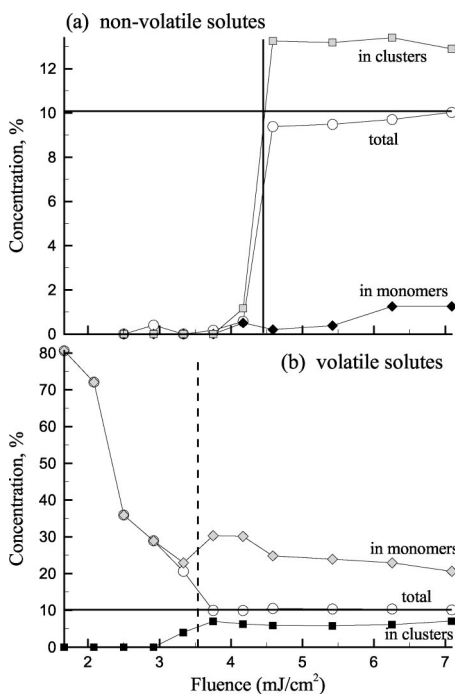


FIG. 3. Concentrations of (a) nonvolatile and (b) volatile solutes ejected as monomers and as a part of the clusters vs laser fluence calculated in molecular dynamics simulations.

is lower than the initial film concentration. As shown in Fig. 3(a), the calculations predict that the nonvolatile solutes preferentially incorporate into the clusters that ablate. In contrast, the volatile solutes [Fig. 3(b)] preferentially ablate as monomers. In the experiments, the presence of clusters can lead to a decrease of ionization efficiency<sup>22,23</sup> and therefore we propose that the ion signals shown in Fig. 2(a) do not reflect the real concentration of  $C_{10}H_{22}$  in the plume in the ablation regime. Other possibilities such as segregation effects in the film and/or in the plume do not seem to be sufficient to account for the difference between the plume and film concentrations.

In conclusion, both the experiments and the simulations of material ejection due to laser irradiation from systems with solutes of different volatility support the existence of two distinct mechanisms of material removal. In particular, the ablation regime can be signified by the ejection of the nonvolatile solutes, whereas the high concentration of the volatile solutes in the plume characterize the desorption regime. Simulations also show that the volatile solutes are ejected mainly as monomers, while the nonvolatile species tend to be incorporated into clusters.

At Penn State University, this work was supported by ONR through the MFEL program. Computational support

was provided by the NSF-MRI program, the IBM-SUR program, and the Center for Academic Computing at PSU. At FORTH, the work was supported by the Large Installations Plan DGXII (Project No. G/89100086/GEP) and by the TMR (No. ERB FMRX-CT98-0188) and fellowships to A.K. and J.L. by EPEAEK programs.

- <sup>1</sup>F. Hillenkamp, M. Karas, R. C. Beavis, and B. T. Chait, *Anal. Chem.* **63**, 1193 (1991).
- <sup>2</sup>A. Piqué, R. A. McGill, D. B. Chrisey, J. H. Callahan, and T. E. Mlsna, *Mater. Res. Soc. Symp. Proc.* **526**, 375 (1998).
- <sup>3</sup>W. A. Tolbert, I.-Y. S. Lee, M. M. Doxtader, E. W. Ellis, and D. D. Dlott, *J. Imaging Sci. Technol.* **37**, 411 (1993).
- <sup>4</sup>L. V. Zhigilei, P. B. S. Kodali, and B. J. Garrison, *Chem. Phys. Lett.* **276**, 269 (1997).
- <sup>5</sup>L. V. Zhigilei and B. J. Garrison, *Appl. Phys. Lett.* **74**, 1341 (1999).
- <sup>6</sup>L. V. Zhigilei and B. J. Garrison, *J. Appl. Phys.* **88**, 1281 (2000).
- <sup>7</sup>K. Dreisewerd, M. Schürenberg, M. Karas, and F. Hillenkamp, *Int. J. Mass Spectrom. Ion Processes* **141**, 127 (1995).
- <sup>8</sup>L. V. Zhigilei, P. B. S. Kodali, and B. J. Garrison, *J. Phys. Chem. B* **101**, 2028 (1997); **102**, 2845 (1998).
- <sup>9</sup>L. V. Zhigilei and B. J. Garrison, *Rapid Commun. Mass Spectrom.* **12**, 1273 (1998).
- <sup>10</sup>L. Dutkiewicz, R. E. Johnson, A. Vertes, and R. Pedrys, *J. Phys. Chem. B* **103**, 2925 (1999).
- <sup>11</sup>M. Handschuh, S. Nettesheim, and R. Zenobi, *Appl. Surf. Sci.* **137**, 125 (1999).
- <sup>12</sup>M. Macler and M. E. Fajardo, *Appl. Phys. Lett.* **65**, 2275 (1994).
- <sup>13</sup>Y. Tsuboi, K. Hatanaka, H. Fukumura, and H. Masuhara, *J. Phys. Chem.* **98**, 11237 (1994).
- <sup>14</sup>S. Georgiou, A. Koubenakis, M. Lassithiotaki, and J. Labrakis, *J. Chem. Phys.* **109**, 8591 (1998).
- <sup>15</sup>A. Koubenakis, T. Elimioti, and S. Georgiou, *Appl. Phys. A: Mater. Sci. Process.* **69**, S637 (1999).
- <sup>16</sup>S. Georgiou, A. Koubenakis, P. Kontoleta, and M. Syrrou, *Chem. Phys. Lett.* **270**, 491 (1997).
- <sup>17</sup>L. V. Zhigilei and B. J. Garrison, *Appl. Phys. A: Mater. Sci. Process.* **69**, S75 (1999).
- <sup>18</sup>A. Koubenakis, J. Labrakis, and S. Georgiou (unpublished).
- <sup>19</sup>A relatively straightforward estimate for comparing the relative fluence values between the experimental and calculated results is to examine the temperature at the surface of the irradiated sample at approximately the ablation threshold. Both systems are in the thermal confinement regime. Ignoring reflection losses,  $T_{\text{final}} = T_{\text{initial}} + F/[LpC\rho]$  where  $F$  is the fluence,  $Lp$  is the penetration depth,  $C$  is the heat capacity, and  $\rho$  is the density. For the experiment with ether,  $C_{\text{ether}} = 1.69 \times 10^3 \text{ J/(K kg)}$  and  $T_{\text{final}} = 100 \text{ K} + 1200 \text{ J/m}^2/[3 \times 10^{-6} \text{ m} \times C_{\text{ether}} \times 0.866 \times 10^3 \text{ kg/m}^3] = 370 \text{ K}$ , a value comparable to the boiling temperature and twice the melting temperature of pure toluene. For the calculation,  $C_{\text{model}} = 4R/(0.100 \text{ kg/mol}) = 0.333 \times 10^3 \text{ J/(K kg)}$  and  $T_{\text{final}} = 0 \text{ K} + 35 \text{ J/m}^2/[55 \times 10^{-9} \text{ m} \times C_{\text{model}} \times 1.21 \times 10^3 \text{ kg/m}^3] = 1600 \text{ K}$ , a value approximately twice the melting temperature of the model system and certainly a temperature where explosive boiling should occur.
- <sup>20</sup>R. Braun and P. Hess, *J. Chem. Phys.* **99**, 8330 (1993).
- <sup>21</sup>P. B. S. Kodali, L. V. Zhigilei, and B. J. Garrison, *Nucl. Instrum. Methods Phys. Res. B* **153**, 167 (1999).
- <sup>22</sup>U. Buck, H. Meyer, D. Nelson, G. Fraser, and W. Klemperer, *J. Chem. Phys.* **88**, 3028 (1988), and references therein.
- <sup>23</sup>T. D. Märk, M. Foltin, M. Kolibar, M. Lezius, and P. Schreiber, *Phys. Scr.*, T **53**, 43 (1994).